

Charge transfer and ionization of lithium by protons and helium ions

R. D. DuBois

Pacific Northwest Laboratory, Richland, Washington 99352

(Received 28 May 1985)

Proton and helium-ion impact on atomic lithium is studied for impact energies ranging from 15 to 200 keV. By observing the final lithium charge states, cross sections for pure single electron capture from lithium as well as for single capture plus ionization are presented. Cross sections for double electron capture by He^{2+} projectiles are also measured and the decrease in the double-capture cross section below 20 keV/amu is confirmed. Cross sections for ionization of lithium by these same projectiles are also presented and compared with theoretical calculations.

INTRODUCTION

Charge transfer occurring in low-energy proton- and α -particle-lithium collisions is of fundamental interest since the outermost $2s$ electron is much more loosely bound than are the $1s$ electrons and therefore single-electron models are applicable. For this reason many experimental and theoretical studies of charge transfer for proton- and helium-ion-lithium collisions have been published in the past few years. Charge-changing collisions with lithium are also of interest because specific reactions have been suggested as a possible means of obtaining a population inversion capable of lasing in the vacuum-ultraviolet or soft-x-ray region or to be useful in diagnosing properties of the hot plasmas produced in thermonuclear fusion reactors. In the latter case the ionization cross sections are also of interest since the proposed method requires injecting neutral lithium beams into the plasma.

In spite of these fundamental and practical interests, until recently¹ no experimental and very little theoretical information concerning the ionization of lithium by proton or helium-ion impact was available. However, sufficient experimental data now exist to provide accurate total single-electron-transfer cross sections from approximately 0.1 to 100 keV/amu (Ref. 2) for H^+ , He^+ , and He^{2+} impact. In the case of double electron capture by α particles, three sets of experimental data exist²⁻⁴ which are in good agreement at energies above 15 keV/amu. Below 15 keV/amu only the data of McCullough *et al.*³ exists. Their data indicate that the double-electron-transfer cross section peaks near 15 keV/amu and then decreases at lower energies. However, the data are subject to large second-order corrections at these lower energies and have not been verified either theoretically or experimentally.

More information about the charge transfer process can be obtained by observing the final projectile and target states. All theoretical treatments of single electron capture by protons or α particles are in agreement that the electron is predominantly captured into excited states of the projectile, namely, into the $n=2$ and 3 levels of the hydrogen atom and into the $n=3$ and 4 levels of the helium ion for lower- and higher-energy collisions, respectively. Cross sections for these processes have been directly

measured for α -particle impact by Barrett and Leventhal⁵ and Kadota *et al.*⁶ In the case of proton impact, Il'in *et al.*⁷ were able to deduce some information about capture into highly excited states of hydrogen, while more recently Aumayr *et al.*⁸ have made direct measurements for capture into the $n=2$ and 3 levels of hydrogen. Information about the final target states formed are limited to an experimental study by Aumayr *et al.*⁹ where they measured lithium excitation occurring for low-energy proton impact. Also Shah *et al.*¹ have just recently reported measurements similar to those presented here.

In order to provide additional information about these collisions, data are presented here where the final lithium-ion charge states resulting from single and double electron capture by protons and helium ions are measured. Cross sections for "pure" electron transfer and for channels where additional ionization accompanies the charge transfer process are presented. *Direct* measurements of double electron transfer are presented where no correction for the competing two-step process was necessary. Last of all, experimental information about the ionization of lithium by proton and helium-ion impact is presented.

EXPERIMENTAL PROCEDURE

The experimental apparatus used for the present work is a modified version of that used previously to study multiple ionization of the rare gases.¹⁰ For the present study the target cell and slow-target-ion detection system were replaced by a stainless-steel metal-vapor oven and a secondary-emission slow-ion detection system modeled after the design of Rinn *et al.*¹¹ A schematic diagram of the apparatus is shown in Fig. 1. As shown, a collimated ion beam crosses the diffuse lithium vapor beam emerging from the oven and is then electrostatically charge analyzed and counted by either of two secondary-emission detectors. These detectors have been previously described in detail (see Ref. 2).

The lithium beam exits the oven through an aperture approximately 1 mm in diameter and 3 mm long. A $2\frac{1}{2}$ -mm-diam aperture in the heat shield and the cooled surface surrounding the interaction region collimate the lithium atoms into a diffuse beam which is collected on liquid-nitrogen-cooled surfaces surrounding the collision

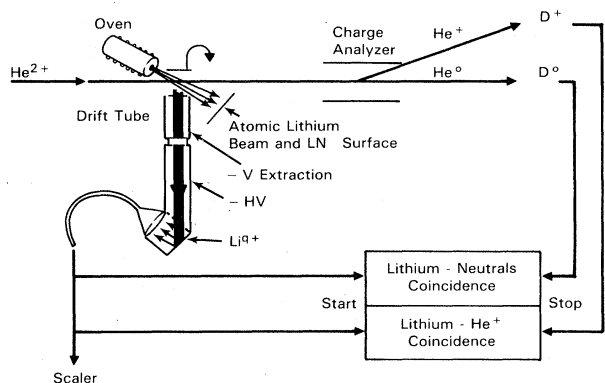
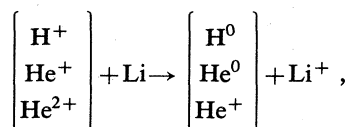


FIG. 1. Schematic diagram of apparatus showing ion beam, atomic-lithium beam, and lithium-ion detection system. D^0 , secondary-emission detector for neutralized beam; D^+ , secondary-emission detector for He^+ (unused for H^+ and He^+ impact). For clarity the oven heat shield and liquid-nitrogen-cooled (LN) surfaces surrounding the interaction region are not shown.

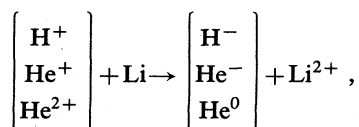
region. The lithium-beam density was estimated to be in the 10^{10} cm^{-3} range by comparing the lithium-ion intensity to that of N_2^+ produced from the background gas. This target density is too low to allow the direct ionization channel to be observed as was done for gaseous targets,¹⁰ but the atomic-beam design was required since all earlier target designs produced extremely high dark counting rates in the slow-ion detector whenever the oven emitted lithium vapor. It is assumed that these dark counts originated from lithium atoms ionizing on the surface of the Channeltron cone since neither bias voltages nor baffles were effective in reducing the dark count. The atomic-beam configuration produced tolerable dark-counting rates for the oven temperatures used in acquiring data.

Target ions, formed by charge transfer and direct ionization, are extracted perpendicular to both the atomic and ion beams by a small (approximately 30 V/cm) electric field. These slow ions of charge q travel through a field-free drift region before being accelerated and counted by a secondary-emission Channeltron detector. The slow lithium ions are produced via single electron capture, double electron capture, capture plus ionization, or direct target ionization, e.g.,

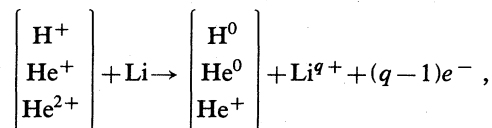
single capture



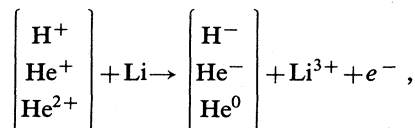
double capture



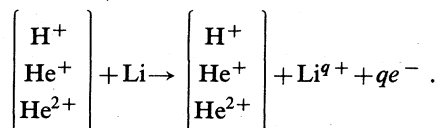
single capture plus ionization ($q=2,3$)



double capture plus ionization



direct ionization ($q=1,2,3$)



Cross sections for the single capture and single capture plus ionization are measured by recording coincidences between the slow target ions and the postcollision neutralized ion beams. These data are recorded and stored in a multichannel analyzer by using standard coincidence electronics and a time-to-amplitude converter. In the case of double capture or double capture plus ionization, only He^{2+} impact was investigated. For these data a second set of coincidence electronics simultaneously records events where He^+ is the final projectile state. Spectra obtained for 200-keV α -particle impact are shown in Fig. 2. Three peaks identifiable as Li^+ , Li^{2+} , and either Li^{3+} or H_2^+ ions, respectively, are observed. A large H_2^+ "contaminant" signal was always observed when initially heating the oven after loading it with lithium—regardless of the procedure used to clean the oven or metal sample. This H_2^+ contaminant slowly became smaller with continued heating and cycling of the oven but never entirely disappeared. Hence it is assumed that H_2^+ and not Li^{3+} is predominantly observed. This may not be the case for the double-capture events observed for He^{2+} impact. Although no cross sections for Li^{3+} are presented for this case, the observed intensities of the Li^{3+} (or H_2^+) ions increased from 1.5% to 9% of the Li^{2+} intensity for double capture by He^{2+} ions with energies from 50 to 200 KeV.

To convert the raw data to absolute cross sections the coincidence data are normalized at each impact energy to

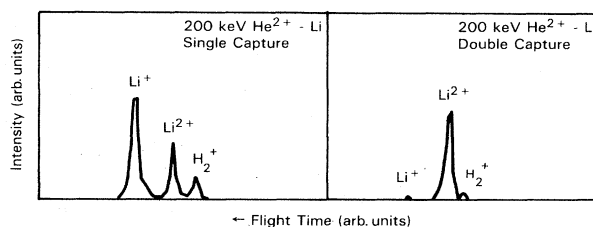


FIG. 2. Lithium-ion charge states observed for 200 keV, ${}^3\text{He}^{2+}$ -Li single- and double-capture collisions. The small peak on the right is assumed to be an H_2^+ impurity and not Li^{3+} (see text for explanation).

single-electron-capture cross sections σ^{10} taken from Ref. 2,

$$\sigma_q^{10} = \sigma^{10} \frac{\text{Li}_q^{10}}{\sum_q \text{Li}_q^{10}}$$

for H^+ and He^+ impact. Here Li_q^{10} are the background-subtracted intensities of the lithium ions having charge q that are created by single electron capture by the projectile. In the designation σ_q^{ij} , i, j are the initial- and final-projectile charge states and q is the residual lithium-ion charge state. For He^{2+} impact the cross sections are determined from

$$\sigma_q^{21} = \sigma^{21} \frac{\text{Li}_q^{21}}{\sum_q \text{Li}_q^{21}}$$

and

$$\sigma^{20} = \sigma^{21} \frac{\sum_q \text{Li}_q^{20}}{\sum_q \text{Li}_q^{21}},$$

where the single-capture cross sections σ^{21} are also taken from Ref. 2. Note that the double-charge-transfer reaction can produce Li^+ ions only if double collisions (the two-step process) occur and hence the present experiment automatically discriminates against that possibility. In addition, any contributions from residual background gases are also observable and can be discriminated against.

In order to obtain information about the direct ionization of lithium a less direct method was used. As already stated the low lithium-beam densities did not permit coincidences between slow target ions and the direct beam to be measured as was done previously for gaseous targets. However by counting all slow target ions produced and subtracting all the charge transfer contributions, it is possible to obtain some information about the ionization of lithium by protons and helium ions. Specifically what is obtained is $\sum_q \sigma_q^{11}$ for H^+ and He^+ impact and $\sum_q \sigma_q^{22}$ for He^{2+} impact. These quantities differ from the "total ionization cross sections" $\sigma_i = \sum_q q \sigma_q^{11}$ or $\sum_q q \sigma_q^{22}$. However, for lithium the amount of multiple ionization should be small enough that $\sum_q q \sigma_q^{nn} \simeq \sum_q \sigma_q^{nn}$.

In order to investigate the efficiency of the slow-target-ion detection system, charge-state ratios (percentage of total charge-state production) were measured using argon as a target. Charge states 1, 2, and 3 were found to be constant within 3% for slow-ion extraction fields ranging from approximately 15 to 90 V/cm. Also it was found that these same fractions were constant within 5% for slow-ion preacceleration voltages between 1.7 and 3.8 kV while maintaining a constant Channeltron gain. Statistical uncertainties were less than 3% for Li^+ production but ranged from 10% to as large as 30% for Li^{2+} production. These combined uncertainties are comparable to the measured reproducibilities which include other factors such as background subtraction. Since the cross sections are normalized at each energy to the single-electron-transfer cross sections taken from Ref. 2, an additional

uncertainty of 15% is assigned. It was shown in Ref. 2 that both beam particle detectors had unit efficiency for higher impact energies and that their detection efficiencies were equal (if not unity) at lower energies. Thus no additional uncertainties are anticipated in determining σ^{20} . Therefore the charge transfer cross sections presented have total absolute uncertainties of approximately 20–30% with perhaps larger errors for the smallest cross sections reported.

The ionization cross sections are subject to uncertainties due to dark-count subtraction (dark counts generally represented less than 15% but occasionally as large as 25% of the total signal), normalization (the ionization signals were 10–40 times larger than the single charge transfer signal which had an absolute uncertainty of 15%), unknown contributions due to ionization of background gases, as well as experimental difficulties encountered for lower impact energies. Thus the ionization results reported here may be accurate only within a factor of 2. This is considered to be a worst-case estimate since subsequent experiments using gaseous targets indicated that the ionization results were accurate to within approximately $\pm 50\%$.

RESULTS

Tabulated cross sections for H^+ , He^+ , and He^{2+} impact are given in Table I while the graphical results are shown in Figs. 3 and 4. Although the data were collected for specific impact energies, they are graphed as a function of impact-velocity squared (keV/amu). This allows an easier comparison of the data for the various projectiles. As shown in Fig. 3 the total single-electron-capture cross section for H^+ and He^+ impact (solid curve) is mainly due to σ_1^{10} , i.e., one electron transfer from lithium to the projectile. This means that, as initially anticipated, lithium simulates a one-electron target very well. At the higher velocities, however, approximately 10% of the time a second electron is ionized as a result of the collision.

The ionization cross sections are considerably larger than the charge transfer cross sections above 20 keV/amu. The measurements agree nicely with the calculation by Olson¹² for proton impact as well as with the calculation for He^+ impact by Tiwary and Rai¹³ above 10 keV/amu. Since submission of this paper Shah *et al.* have reported¹ ionization cross sections for H^+ -Li collisions. A preliminary comparison of their cross sections with the present data indicate good agreement in the overlapping energy range. Also shown for comparison are the electron-impact measurements of McFarland and Kinney¹⁴ and Zapesochnyi and Aleksakhin¹⁵ which seem to merge with the present results at higher energies. Note that both experiment and theory imply that the ionization cross sections are the same for equal velocity proton and helium-ion impact.

The results for α -particle impact (Fig. 4) show that at higher impact energies approximately a third of the single-electron-transfer collisions also result in ionization of a second electron from lithium. This process is larger than the direct capture of two electrons by the projectile.

The double-electron-capture cross section is compared with previous measurements that were made using the growth-curve method. The present data confirm that the cross section peaks near 20 keV/amu and then decreases sharply at lower energies. Since the Li^{3+} contribution was not included, the present double-electron-capture cross sections should be slightly smaller than the previous measurements (by 1.5% to 9% according to the discus-

sion given earlier in this paper); however, they are approximately 30–40% larger. The present technique also yielded larger double-electron-transfer cross sections for other metal-vapor and gaseous targets than those measured by the growth-curve method. No experimental reason for this discrepancy has been found.

The ionization cross sections again exceed the charge transfer cross sections at higher energies and again agree well with the calculation of Olson.¹² As was the case for H^+ impact, a preliminary comparison of the present data and the recent data of Shah *et al.*¹ yields good agreement.

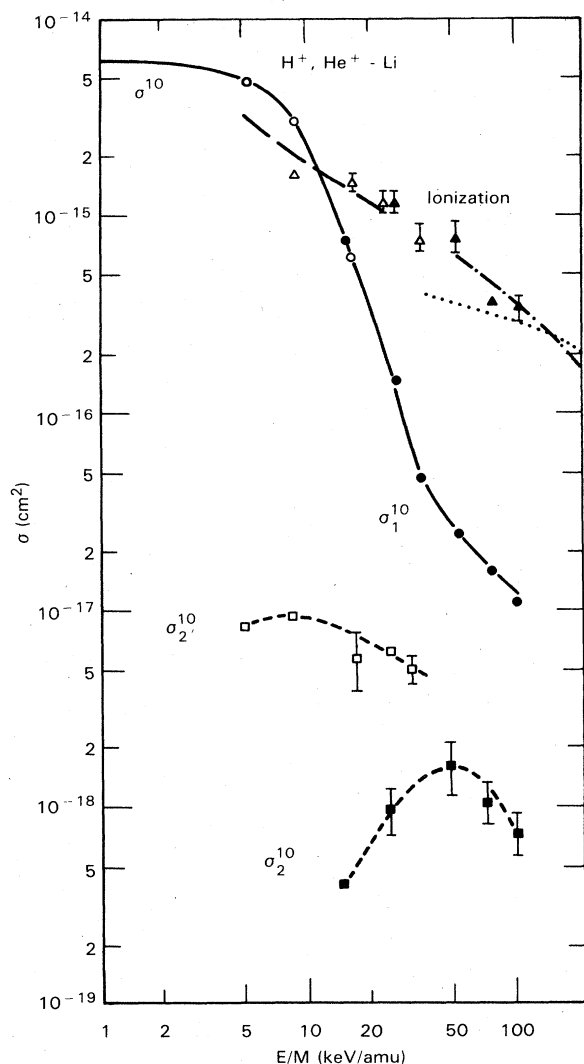


FIG. 3. Cross sections for charge transfer and ionization of lithium by H^+ and He^+ impact. Charge transfer: —, total single-charge-transfer cross section σ^{20} obtained from smooth curve through data in Ref. 2; ●, σ_1^{10} for H^+ impact; ○, σ_1^{10} for He^+ impact; ■, σ_2^{10} for H^+ impact; □, σ_2^{10} for He^+ impact. Dashed curves through the data points are to guide the eye. Ionization: ▲, $\sum_q \sigma_q^{11}$ for H^+ impact; △, $\sum_q \sigma_q^{11}$ for He^+ impact; - - - - -, ionization-cross-section calculation for H^+ impact (Ref. 12); - - - - -, ionization-cross-section calculation for He^+ impact (Ref. 13); ····, electron-impact-ionization cross sections (Refs. 14 and 15). Error bars are for experimental reproducibility only.

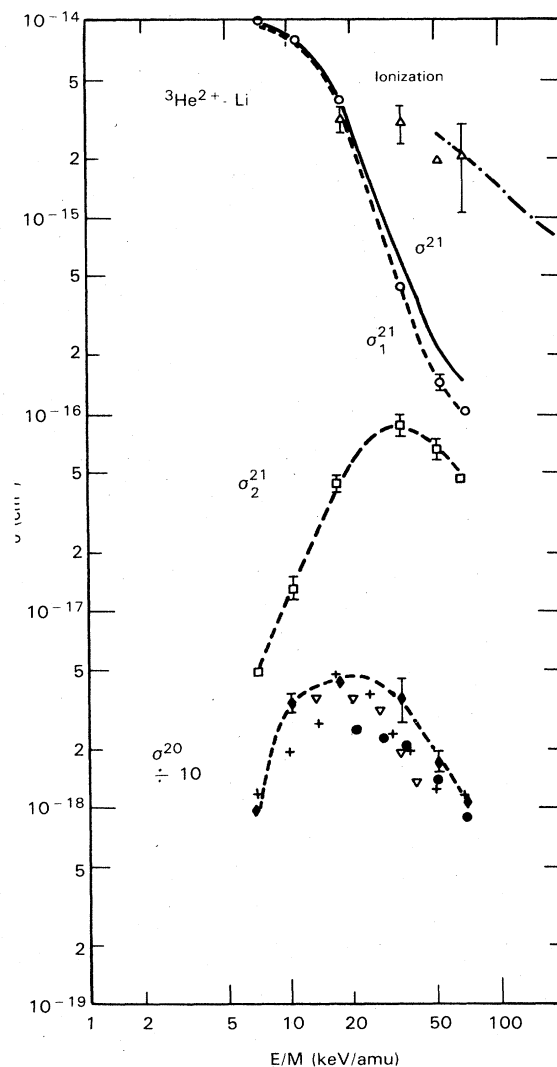


FIG. 4. Cross sections for charge transfer and ionization of lithium by He^{2+} impact. Charge transfer: —, total charge-transfer cross section σ^{21} obtained from smooth curve through data of Ref. 2; ○, σ_1^{21} ; □, σ_2^{21} ; ◆, present σ_2^{20} measurements; ●, σ^{20} from Ref. 2; +, σ^{20} from Ref. 3; ▽, σ^{20} from Ref. 4. Dashed curves through the present data are to guide the eye. Ionization: △, present $\sum_q \sigma_q^{22}$ measurements; - - - - -, ionization-cross-section calculation of Ref. 12. Error bars are for experimental reproducibility only.

TABLE I. Absolute cross sections in (units of 10^{-16} cm²) for charge transfer and ionization of lithium by H⁺, ³He⁺, and ³He²⁺. Superscripts represent the projectile pre- and postcollision charge states and the subscript is the final lithium-ionization charge state. Errors are experimental reproducibility only.

Projectile <i>E/M</i> (keV/amu)	H ⁺			³ He ⁺			³ He ²⁺			
	σ_1^{10}	σ_2^{10}	$\sum_q \sigma_q^{11}$	σ_1^{10}	σ_2^{10}	$\sum_q \sigma_q^{11}$	σ_1^{21}	σ_2^{21}	σ^{20}	$\sum_q \sigma_q^{22}$
100	0.114	0.0075	3.5							
		±0.0018	±0.5							
75	0.159	0.0108	3.71							
		±0.0027	±0.06							
66.7							1.03	0.467	0.108	20.1
								±0.008	±0.013	±10.1
50	0.254	0.0164	7.9				1.43	0.67	0.173	19.3
		±0.0057	±1.4				±0.09	±0.09	±0.018	±1.1
33.3				0.489	0.051	7.8	4.53	0.874	0.362	29.9
					±0.008	±1.3	±0.10	±0.095	±0.087	±7.3
25	1.49	0.0098	12.0	1.44	0.0626	12.0				
		±0.0027	±1.4		±0.0003	±1.3				
16.7				6.24	0.06	15.1	39.6	0.450	0.440	31.5
					±0.02	±1.6		±0.037	±0.006	±4.8
15	7.76	0.0406								
10							77.8	0.132	0.338	
								±0.023	±0.026	
8.33				32	0.0096	16.6				
6.67							98.0	0.0495	0.0966	
								±0.0035	±0.0021	
5				48.9	0.0833					

Also note that the present ionization cross sections for He²⁺ impact are approximately four times larger than those for H⁺ impact as is expected.

CONCLUSIONS

Cross sections for charge transfer in lithium-proton and lithium-helium ion collisions have been presented where, for the first time, the final charge state of lithium has been observed. It was found that the charge transfer process for H⁺ and He⁺ impact is predominantly "pure," i.e., additional ionization is rare. However, additional ionization of one electron occurs approximately 30% of the

time for higher-energy α -particle impact. The present double-electron-transfer measurements have verified that the cross section decreases below 20 keV/amu. Last of all, experimental measurements of the ionization of lithium by ion impact were presented and shown to agree well with existing ionization calculations as well as with recent measurements.

ACKNOWLEDGMENT

This work was supported by the U. S. Department of Energy, Division of Magnetic Fusion Energy, Contract No. DE-AC06-76RLO-1830.

- ¹M. B. Shah, D. S. Elliott, and H. B. Gilbody, in *Proceedings of the XIVth International Conference on the Physics of Electronic and Atomic Collisions, Stanford, 1985*, edited by M. J. Coggiola, D. L. Huestis, and R. P. Saxon (ICPEAC, Stanford, 1985), p. 405.
- ²R. D. DuBois and L. H. Toburen, *Phys. Rev. A* **31**, 3603 (1985).
- ³R. W. McCullough, T. V. Goffe, M. G. Shah, M. Lennon, and H. B. Gilbody, *J. Phys. B* **15**, 111 (1982).
- ⁴G. A. Murray, J. Stone, M. Mayo, and T. J. Morgan, *Phys. Rev. A* **25**, 1805 (1982).
- ⁵J. L. Barrett and J. J. Leventhal, *Phys. Rev. A* **23**, 485 (1981).
- ⁶K. Kadota, D. Dijkkamp, R. Van der Woude, Pan Guang Yan, and F. J. DeHeer, *Phys. Lett.* **88A**, 135 (1982).
- ⁷R. N. Il'in, V. A. Oparin, E. S. Solovev, and N. V. Federenko,

Zh. Tekh. Fiz. **36**, 1241 (1966) [*Sov. Phys.—Tech. Phys.* **11**, 921 (1967)].

- ⁸F. Aumayr, M. Fehring, and H. Winter, *J. Phys. B* **17**, 4201 (1984).
- ⁹F. Aumayr, M. Fehring, and H. Winter, *J. Phys. B* **17**, 4185 (1984).
- ¹⁰R. D. DuBois, *Phys. Rev. Lett.* **52**, 2348 (1984).
- ¹¹K. Rinn, A. Müller, H. Eichenauer, and E. Salzborn, *Rev. Sci. Instrum.* **53**, 829 (1982).
- ¹²R. E. Olson, *J. Phys. B* **15**, L163 (1982).
- ¹³S. N. Tiwary and D. K. Rai, *J. Chem. Phys.* **68**, 2427 (1978).
- ¹⁴R. H. McFarland and J. D. Kinney, *Phys. Rev. A* **137**, 1058 (1965).
- ¹⁵I. P. Zapesochnyi and I. S. Aleksakhin, *Zh. Eksp. Teor. Fiz.* **55**, 76 (1968) [*Sov. Phys.—JETP* **28**, 41 (1969)].